

# Temperature-Programmed Desorption of Pyridine on Silica Overlayers Deposited on ZrO<sub>2</sub> and TiO<sub>2</sub> by Chemical Vapor Deposition of Si(OC<sub>2</sub>H<sub>5</sub>)<sub>4</sub>

T. Jin, S. K. Jo, C. Yoon, and J. M. White\*

Department of Chemistry and Center for Materials Chemistry, University of Texas, Austin, Texas 78712

Received December 16, 1988

Silica overlayers deposited on ZrO<sub>2</sub> and TiO<sub>2</sub> by chemical vapor deposition of Si(OC<sub>2</sub>H<sub>5</sub>)<sub>4</sub> have been characterized by using temperature-programmed desorption of pyridine and Auger electron spectroscopy (AES). On ZrO<sub>2</sub>, the pyridine uptake decreased slowly with silica deposition until the silica fraction (Si/(Si + Zr)) reached 40%; then it decreased strongly with further deposition. On TiO<sub>2</sub>, with silica deposition pyridine adsorption also decreased slowly up to an AES silica fraction of 45%. With additional deposition of silica, the pyridine uptake then remained constant. These results agree with our previous conclusion that a thin SiO<sub>x</sub> film covering the entire substrate was formed on ZrO<sub>2</sub> and that a mixed oxide layer was formed on TiO<sub>2</sub>.

## Introduction

Preparation of metal oxide thin films by chemical vapor deposition (CVD) of organometallic molecules has been common in such fields as solar energy conversion,<sup>1,2</sup> corrosion protection,<sup>3</sup> electronic devices,<sup>4,5</sup> chemical sensors,<sup>6</sup> and catalysis.<sup>7-9</sup> In catalysis, for example, CVD has been used in preparing model catalysts with interesting properties, e.g., mixing two different oxides often results in the generation of new acidic sites.<sup>10</sup> In mixed oxides containing SiO<sub>2</sub> (Al<sub>2</sub>O<sub>3</sub>-SiO<sub>2</sub>, for instance), Brønsted acid sites are believed to be formed on SiO<sub>2</sub> and Lewis acid sites on the other component.<sup>10</sup> Preparation of a uniform thin silica film on a second oxide support might result in only Brønsted sites on the surface, providing a good model for studying oxide interactions.

Imizu et al.<sup>9</sup> reported that silica, which is normally inactive for chemisorption of pyridine, was activated by its deposition on MgO. However, the morphology of the silica overlayer has not been investigated. In previous work from our laboratory,<sup>11,12</sup> a morphological study of silica overlayers derived from Si(OC<sub>2</sub>H<sub>5</sub>)<sub>4</sub> vapor-deposited on ZrO<sub>2</sub> and TiO<sub>2</sub> was carried out by using ISS, AES, and Ar<sup>+</sup> sputtering depth profiles. The results indicate that on ZrO<sub>2</sub>, Si(OC<sub>2</sub>H<sub>5</sub>)<sub>4</sub> decomposed to form a thin SiO<sub>x</sub> film, whereas on TiO<sub>2</sub>, it formed a mixed oxide layer. For both, very little C was retained, but somewhat more was retained on TiO<sub>2</sub>. In the present study, the chemical properties of the silica overlayers have been examined by using temperature-programmed desorption (TPD) of pyridine. Our results support previously proposed models for overlayer morphology.

## Experimental Section

The ultrahigh vacuum (UHV) system for TPD and AES was similar to that described elsewhere.<sup>13,14</sup> It consisted of two

chambers, one for dosing and reaction and the other for TPD and AES analysis. A differentially pumped and sealed polished rod was used to transport the sample between the chambers. Base pressures in both chambers with  $5 \times 10^{-9}$  Torr. Tetraethoxysilane (Si(OC<sub>2</sub>H<sub>5</sub>)<sub>4</sub>) was introduced only into the dosing chamber.

ZrO<sub>2</sub>, obtained by calcination at 840 K of Zr(OH)<sub>4</sub> and prepared from zirconium nitrate, and TiO<sub>2</sub> (Degussa) had surface areas of 50 m<sup>2</sup>/g as measured by N<sub>2</sub> adsorption. As previously described,<sup>14,15</sup> the oxide substrates were mounted by pressing the powders into a 1-cm<sup>2</sup> Ta mesh that had been spot welded over two tantalum heater leads. The temperature was monitored by a chromel-alumel thermocouple also spot welded on the Ta mesh. The highest temperature reached was 900 K. Prior to TPD experiments, the samples were evacuated at 800 K for 20 min to remove the adsorbed water and carbon monoxide.

Si(OC<sub>2</sub>H<sub>5</sub>)<sub>4</sub> (99.999%, Alfa Products) was introduced as a gas into the dosing-reaction chamber through a reentrant Pyrex tube that passed through the vacuum chamber wall with a glass-to-metal seal. The end of this tube was located about 10 mm from the sample. The liquid alkoxide source was contained in an external Pyrex tube separated from the UHV system by two greaseless stopcocks. Si(OC<sub>2</sub>H<sub>5</sub>)<sub>4</sub> was dosed in cycles (10<sup>-5</sup> Torr, 300 K, 10 min), each of which was followed by flash heating to 773 K.

## Results

**Thermal Decomposition of Si(OC<sub>2</sub>H<sub>5</sub>)<sub>4</sub>.** Silica was deposited on ZrO<sub>2</sub> and TiO<sub>2</sub> by repeated cycles of dosing and thermal decomposition. Each dosing cycle was followed by AES measurement and pyridine TPD to determine the correlation between surface silica coverage and chemisorption properties. Gas-phase Si(OC<sub>2</sub>H<sub>5</sub>)<sub>4</sub> gives a number of fragments in mass spectra, the major ones, in order of intensity, being at *m/e* 149, 79, 119, and 163. In the present study, mass numbers 28, 45, and 79 were monitored in TPD for expected decomposition products, ethylene and ethanol, and undecomposed Si(OC<sub>2</sub>H<sub>5</sub>)<sub>4</sub>. Domination by ethylene of mass 28 was confirmed by following masses 26 and 27 in some experiments.

TPD of Si(OC<sub>2</sub>H<sub>5</sub>)<sub>4</sub> dosed onto ZrO<sub>2</sub>, TiO<sub>2</sub>, and SiO<sub>2</sub> confirmed earlier data obtained from mass signals 27 and 163.<sup>16</sup> Only the desorption of undecomposed Si(OC<sub>2</sub>H<sub>5</sub>)<sub>4</sub> was observed for a bulk SiO<sub>2</sub> substrate at 390 K. In our earlier work, desorption peaks of *m/e* 163, 27, and 18 were observed at 550-650 K.<sup>16</sup> These peaks were identified as

- (1) Pettit, R. B.; Brinker, C. J. *SPIE* 1985, 562, 256.
- (2) Pettit, R. B.; Brinker, C. J.; Ashley, C. S. *Sol. Cells* 1985, 15, 267.
- (3) *Chem. Eng. News* 1986, Aug 11, 22.
- (4) Kojima, Y.; Kamiya, M.; Tanaka, K.; Nagaai, K.; Hayashi, Y. *Int. Electron. Device Meeting* 1981, 388.
- (5) Liang, M.; Hu, C. *Int. Electron. Device Meeting* 1981, 396.
- (6) Carlson, T.; Griffin, G. L. *J. Phys. Chem.* 1986, 90, 5896.
- (7) Asokura, K.; Iwasawara, Y.; Kuroda, H. *Shokubai* 1985, 27, 371.
- (8) Niwa, M.; Kata, M.; Hattori, T.; Murakami, Y. *J. Phys. Chem.* 1986, 90, 6233.
- (9) Imizu, Y.; Tada, A.; Tanaka, K.; Toyoshima, I. *Shokubai* 1987, 29, 98.
- (10) Tanabe, K. *Catalysis—Science and Technology*; Anderson, J. R.; Boudart, M., Eds.; Springer-Verlag: Berlin, 1981; Vol. 2, p 231.
- (11) Jin, T.; Okuhara, T.; White, J. M. *J. Chem. Soc., Chem. Commun.* 1987, 1248.
- (12) Jin, T.; White, J. M. *Surf. Interface Anal.* 1988, 11, 517.

- (13) Beck, D. D.; White, J. M. *J. Phys. Chem.* 1984, 88, 2764.
- (14) Henderson, M. A.; Jin, T.; White, J. M. *Appl. Surf. Sci.* 1986, 27, 127.
- (15) Jin, T.; Okuhara, T.; Mains, G. J.; White, J. M. *J. Phys. Chem.* 1987, 91, 3310.
- (16) Okuhara, T.; White, J. M. *Appl. Surf. Sci.* 1987, 29, 223.

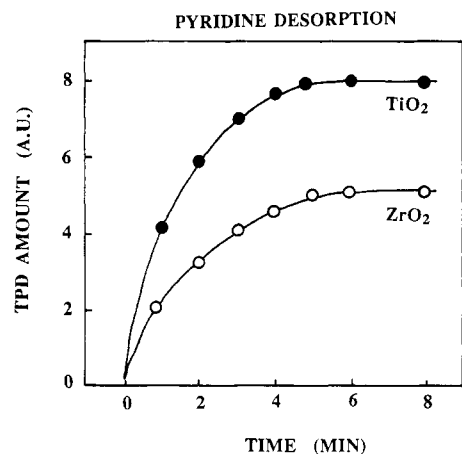


**Figure 1.** TPD peak areas versus dose time for pyridine dosed on  $ZrO_2$  (○) and  $TiO_2$  (●) at 300 K and  $10^{-4}$  Torr.

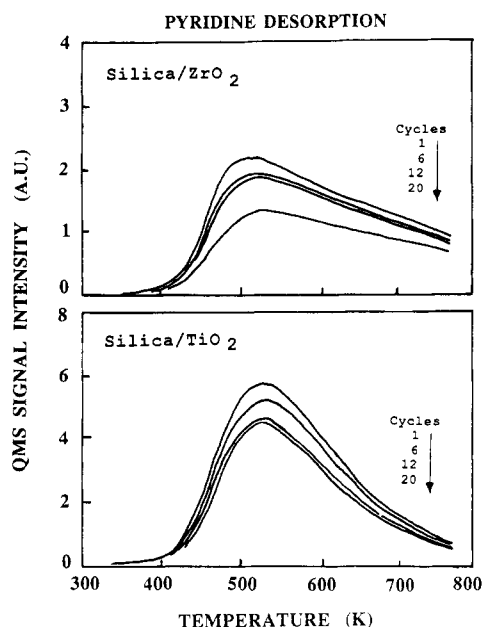


**Figure 2.** TPD profiles for pyridine desorption from silica-covered zirconia (upper panel) and titania (lower panel). The four curves in each of the two panels correspond to different numbers of cycles of dosing  $Si(OC_2H_5)_4$  (see text). From top-to-bottom in each panel: first, sixth, twelfth, and twentieth dose.

desorption and decomposition of  $Si(OC_2H_5)_4$  condensed on the copper block<sup>14</sup> when liquid nitrogen was used for cooling. For  $ZrO_2$  and  $TiO_2$ , significant desorption of ethylene (28 amu) was observed at 590 and 640 K, respectively. The desorption peaks for mass 79 ( $Si(OH)_3^+$ ) and 45 ( $OC_2H_5^+$ ) were negligible for both substrates. Besides ethylene, water was the only significant desorption product, and it desorbed above 700 K.

Molecular ethylene was dosed on  $ZrO_2$  and  $TiO_2$  ( $10^{-5}$  Torr, 2 min) at 300 K. On  $ZrO_2$ , ethylene desorbed at 330 K. No significant desorption was observed on  $TiO_2$ .

**TPD of Pyridine.** Temperature-programmed desorption (TPD) of pyridine was carried out after each  $Si(OC_2H_5)_4$  deposition cycle. Pure  $SiO_2$  (Cab-O-sil) did not show any desorption when pyridine was dosed at 423 K. Figure 1 plots the TPD peak area of pyridine dosed on  $ZrO_2$  and  $TiO_2$  at 423 K vs exposure. Saturation was reached with a pyridine exposure of  $10^{-4}$  Torr for 5 min. Figure 2 shows the TPD profiles of saturation pyridine (based on the parent fragment) dosed on  $ZrO_2$  and  $TiO_2$  after the first, sixth, twelfth, and twentieth  $Si(OC_2H_5)_4$  deposition cycles. For both substrates, pyridine desorbed

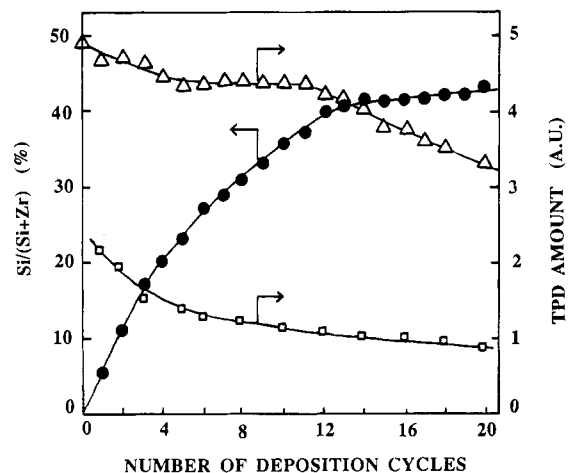


**Figure 3.** Surface composition by AES and TPD peak areas as a function of the number of  $Si(OC_2H_5)_4$  doses on  $ZrO_2$ : (●) calibrated AES peak-to-peak height ratio,  $Si/(Si + Zr)$ ; (Δ) ethylene TPD peak area; (□) pyridine TPD peak area.

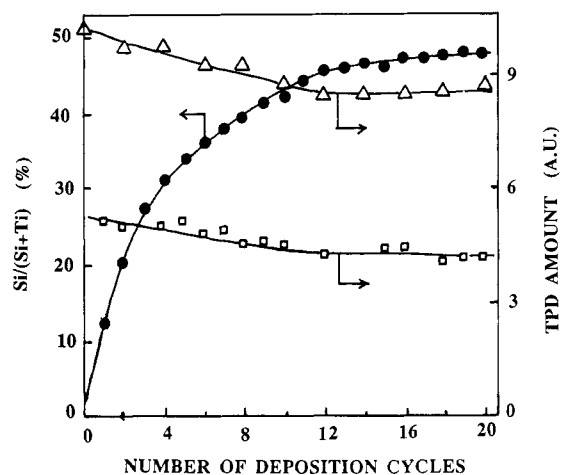


**Figure 4.** Surface composition by AES and TPD peak areas as a function of the number of  $Si(OC_2H_5)_4$  doses on  $TiO_2$ : (●) calibrated AES peak-to-peak height ratio,  $Si/(Si + Zr)$ ; (Δ) ethylene TPD peak area; (□) pyridine TPD peak area.

in broad peaks, indicating that the adsorption sites are heterogeneous. The amount of desorbed pyridine decreased as the amount of silica deposited increased. The rate of decrease after the twelfth  $Si(OC_2H_5)_4$  deposition cycle became higher for  $ZrO_2$ , but not for  $TiO_2$ .

**Surface Composition and Amounts of Pyridine Adsorbed.** To correlate the amount of  $SiO_2$  deposited with the pyridine TPD area and with the amount of ethylene arising from  $Si(OC_2H_5)_4$  decomposition, Auger electron spectra of the samples were recorded after each silica deposition cycle. Figures 3 and 4 summarize the surface fraction of Si for  $ZrO_2$  and  $TiO_2$ , respectively. The relative AES sensitivities of Si (91 eV), Zr (147 eV), and Ti (396 eV) are based on handbook values.<sup>17</sup> TPD amounts are normalized to the sample weights of  $ZrO_2$  and  $TiO_2$ .

For the first few cycles and for both substrates, the fraction of silica,  $Si/(Si + Zr)$  or  $Si/(Si + Ti)$ , increased rapidly. After about 12 cycles, the rate of growth slowed, and the Si fraction stabilized at 41% for  $ZrO_2$  and 46% for  $TiO_2$ .

Figures 3 and 4 also show that the pyridine uptake decreased with the number of the dosing cycles of  $Si(OC_2H_5)_4$ .

(17) Davis, L. E.; McDonald, N. C.; Riach, G. E.; Weber, R. E. *Handbook of Auger Electron Spectroscopy*; Physical Electronics: Edina, MN, 1976.

For  $ZrO_2$ , the decrease was slow through the first 12  $Si(OC_2H_5)_4$  deposition cycles, but further cycles led to a more rapid decrease (Figure 3). In the case of  $TiO_2$ , however, the TPD amount of pyridine decreased steadily during the initial cycles but remained steady after the twelfth dosing cycle (Figure 4).

The amount of ethylene desorbed versus the number of dosing cycles differs for the two supports. For  $ZrO_2$ , after 20 deposition cycles ( $10^{-5}$  Torr, 300 K, 10 min, followed by flash heating) the TPD peak area decreased about 60% (Figure 3), while in the case of  $TiO_2$ , the decrease was less than 30% (Figure 4).

### Discussion

Recent ion scattering spectroscopy work<sup>11,12</sup> showed that as the AES fraction of silica approached 40% during CVD of  $Si(OC_2H_5)_4$ , the  $ZrO_2$  surface was more than 90% covered with silica. The  $TiO_2$  surface, on the other hand, was never more than 70% covered, even though the AES fraction reached 45–50%. The present AES data (Figures 3 and 4) are in close accord.

The TPD results (Figure 4), however, show that the amount of ethylene desorbing from  $Si(OC_2H_5)_4$  remains high for  $TiO_2$  even after the silicon fraction in the surface layer stops rising. This indicates continued silicon ethoxide decomposition even after reaching maximum coverage (70%<sup>11,12</sup>) of the  $TiO_2$  surface. TPD of pyridine (Figures 2 and 4) also shows a constant peak area after the twelfth dosing cycle, indicating that pyridine uptake is not affected by additional silica deposition. TPD of both ethylene (from  $Si(OC_2H_5)_4$ ) and pyridine strongly suggests that the structural and chemical properties of the top layer are not changed by further deposition of silica. As noted earlier, bulk  $SiO_2$  adsorbs no pyridine at 423 K. However, it has been reported that mixing  $TiO_2$  with  $SiO_2$  (by coprecipitation) results in the generation of acidic sites<sup>18</sup> which do adsorb pyridine. The present results are consistent with a model<sup>12</sup> wherein  $Si(OC_2H_5)_4$  decomposes on  $TiO_2$  to form a mixed oxide layer, probably including  $SiO_2$  islands or clusters. Beyond a certain number of cycles, the chemical composition of the mixed oxide layer does not change significantly during deposition of silica. This mixed layer retains sufficient acidity to adsorb pyridine.

In the case of  $ZrO_2$ , ISS<sup>12</sup> shows that the substrate was fully covered as the AES fraction of silica ( $Si/(Si + Zr)$ ) reached 40%. The pyridine uptake, however, decreased only slightly under these conditions (12 decomposition cycles of Figure 3). We conclude that the supported thin-film silica, prepared by CVD of  $Si(OC_2H_5)_4$ , differs

significantly from bulk  $SiO_2$ , which does not chemisorb pyridine. In these thin films over  $ZrO_2$ , silica shows significant chemisorption activity for *basic* molecules. The activation of the silica by the  $ZrO_2$  support may be due to a charge redistribution.<sup>9,10,19,20</sup> The latter could occur if the thin layer of surface silica followed the atomic arrangement and spacing of  $ZrO_2$ .

Since the surface of  $ZrO_2$  was completely covered after the twelfth dosing cycle (Figure 3), any further silica deposition is believed to build up a second layer and/or islands on the first layer.<sup>12</sup> The strong decrease in pyridine uptake after the twelfth silica deposition cycle (Figure 3) is consistent with this model.<sup>12</sup> As the silica overlayer becomes thicker, its chemical properties are more like those of bulk  $SiO_2$ .

Decomposition of  $Si(OC_2H_5)_4$  over various metal oxides has been discussed previously.<sup>16</sup> Since directly introducing ethylene to  $ZrO_2$  and  $TiO_2$  did not result in ethylene desorption above 500 K, the temperature of the ethylene desorption from  $Si(OC_2H_5)_4$  must reflect the  $Si(OC_2H_5)_4$  decomposition temperature. The fact that ethylene from  $Si(OC_2H_5)_4$  desorbed at a lower temperature from  $ZrO_2$  than from  $TiO_2$  may suggest that  $ZrO_2$ , with acid-base bifunctional sites,<sup>10</sup> is more favorable for  $Si(OC_2H_5)_4$  decomposition than the more acidic  $TiO_2$ .<sup>10,21</sup>

### Summary

1. Unlike bulk  $SiO_2$ , silica thin films deposited on  $ZrO_2$  by CVD of  $Si(OC_2H_5)_4$  are active for pyridine chemisorption, indicating that acidic sites are generated on the supported silica film.

2. On  $ZrO_2$ , the amount of chemisorbed pyridine decreases sharply as the silica film thickness increases beyond completion of the first layer.

3. On  $TiO_2$ , the amount of chemisorbed pyridine first drops as  $SiO_2$  is added but then becomes independent of further silica deposition.

4. Observations 2 and 3 above support the formation of silica overlayer films on  $ZrO_2$  and mixed oxide layers on  $TiO_2$ .

**Acknowledgment.** Support by the Robert A. Welch Foundation and the Texas Advanced Technology Research Program is gratefully acknowledged.

**Registry No.**  $SiO_2$ , 7631-86-9;  $ZrO_2$ , 1314-23-4;  $TiO_2$ , 13463-67-7;  $Si(OC_2H_5)_4$ , 78-10-4; pyridine, 110-86-1.

(19) Seiyama, M. *Metal Oxides and Their Catalytic Actions*; Kodasha Scientific: Tokyo, 1978.

(20) Thomas, C. L. *Ind. Eng. Chem.* **1949**, *41*, 2564.

(21) Jin, T.; Hattori, H.; Tanabe, K. *Bull. Chem. Soc. Jpn.* **1983**, *56*, 3206.

(18) Itoh, M.; Hattori, H.; Tanabe, K. *J. Catal.* **1974**, *35*, 225.